Electronic Texture of the Thermoelectric Oxide $Na_{0.75}CoO_2$

M.-H. Julien,[1,*] C. de Vaulx,[1] H. Mayaffre,[1] C. Berthier,[1,2] M. Horvatić,[2] V. Simonet,[3] J. Wooldridge,[4] G. Balakrishnan,[4] M. R. Lees,[4] D. P. Chen,[5] C. T. Lin,[5] and P. Lejay[3]

[1]*Laboratoire de Spectrométrie Physique, UMR5588 CNRS and Université J. Fourier-Grenoble, 38402 Saint Martin d'Hères, France*
[2]*Grenoble High Magnetic Field Laboratory, CNRS, BP166, 38042 Grenoble, France*
[3]*Institut Néel, CNRS/UJF, BP166, 38042 Grenoble Cedex 9, France*
[4]*Department of Physics, University of Warwick, Coventry CV4 7AL, United Kingdom*
[5]*Max-Planck-Institut for Solid State Research, Heisenbergstrasse 1, 70569 Stuttgart, Germany*

(Received 4 December 2007; published 5 March 2008)

From ^{59}Co and ^{23}Na NMR, we demonstrate the impact of the Na^+ vacancy ordering on the cobalt electronic states in $Na_{0.75}CoO_2$: at long time scales, there is neither a disproportionation into 75% Co^{3+} and 25% Co^{4+} states, nor a mixed-valence metal with a uniform $Co^{3.25+}$ state. Instead, the system adopts an intermediate configuration in which 30% of the lattice sites form an ordered pattern of localized Co^{3+} states. Above 180 K, an anomalous mobility of specific Na^+ sites is found to coexist with this electronic texture, suggesting that the formation of the latter may contribute to stabilizing the Na^+ ordering. Control of the ion doping in these materials thus appears to be crucial for fine-tuning of their thermoelectric properties.

DOI: 10.1103/PhysRevLett.100.096405 PACS numbers: 71.28.+d, 72.15.Jf, 75.20.−g, 76.60.−k

Complexity, which underlies many physical properties of correlated electron systems [1], often results from the spatial modulation of electronic states. Besides the tendency to form ordered patterns (such as stripes in high temperature superconductors), electrostatic interactions with dopant ions are increasingly recognized as a source of electronic inhomogeneity [2,3]. Because the sodium ions in Na_xCoO_2 are mobile and can order, these battery materials are emerging as exceptional candidates for exploring such phenomena [4]. One of the most important questions regarding this system is whether the intriguing physical properties of metallic phases at $x \gtrsim 0.6$ are related to a coupling between the electronic degrees of freedom and the spatial distribution of Na^+ vacancies [4–13]. On the one hand, long range sodium vacancy ordering has been reported, but the ordering pattern appears to be controversial for the most studied concentration $x = 0.75$ [13–15]. On the other hand, electronic ''textures,'' which may be defined as both the disproportionation of electronic (spin, charge, and possibly orbital) states and the spatial correlation between these states, are much less experimentally accessible and, not surprisingly, no electronic pattern has yet been resolved. Nevertheless, the observation of two, or more, magnetically distinct ^{59}Co sites at the time scale ($\sim 10^{-6}$ s) of nuclear magnetic resonance (NMR) [16–21] demonstrates that some electronic disproportionation occurs in metallic Na_xCoO_2 with $x \sim 0.7$. However, because of the difficulty in accurately determining the Na content x, and the sensitivity of Na order to small variations in x or to the synthesis method, a coherent picture of the electronic states has yet to emerge.

We have obtained reproducible NMR spectra of ^{59}Co nuclei in high quality single crystals of $Na_{0.75}CoO_2$, grown in three different groups [22,23]. Our comprehensive characterization of the crystals will be published separately. For the magnetic field $H \parallel c$ (i.e., $\theta = 0°$), a typical spectrum (Fig. 1) shows three distinct sites. These are labeled Co1, Co2, and Co3 in increasing order of their magnetic hyperfine shift $K = K^{\rm orb} + K^{\rm spin}$. The most interesting differences between these sites lie in both (i) the value of the on site orbital contribution $K^{\rm orb}$, which is proportional to the (on site) Van Vleck susceptibility, and (ii) the value of $K^{\rm spin}$ (''Knight shift'' in metals), which for a given nuclear site i is given by

$$K^{\rm spin}_{\alpha\alpha,i} = A_{\alpha\alpha}\frac{\chi^{\rm spin}_{\alpha\alpha}(i)}{g\mu_B} + \sum_j B\frac{\chi^{\rm spin}_{\alpha\alpha}(j)}{g\mu_B}, \qquad (1)$$

where A is the on site hyperfine coupling, $\chi^{\rm spin}$ is the local spin susceptibility, and j stands for the nearest Co neighbors to which the nucleus i may be coupled *via* a transferred hyperfine interaction B. $\alpha = c, ab$ is the direction of the principal axis of A and χ tensors, along which H is aligned. Equation (1) makes clear that, if $B \neq 0$ and $\chi^{\rm spin}(i) \neq \chi^{\rm spin}(j)$, the number of NMR sites with different $K^{\rm spin}(i)$ values may be greater than the number of different magnetic sites [i.e., of different $\chi(i)$ values]. Thus, the three ^{59}Co NMR sites do not necessarily correspond to three distinct electronic densities.

Additional information on the cobalt sites is provided by the anisotropy and the temperature (T) dependence of K. $H||ab$ spectra are too poorly resolved to directly extract the in-plane anisotropy and the K values for all sites. Nevertheless, neglecting the in-plane anisotropy, K_{ab} can be extracted from a combined knowledge of the line positions for $\theta = 54.7°$ and $\theta = 0°$, which define $K_{\rm iso} = \frac{1}{3} \times (2K_{ab} + K_c)$ and K_c, respectively. The values of $K^{\rm orb}$ and of the effective total hyperfine field $\mathcal{A}^{\rm hf}$ for each site are

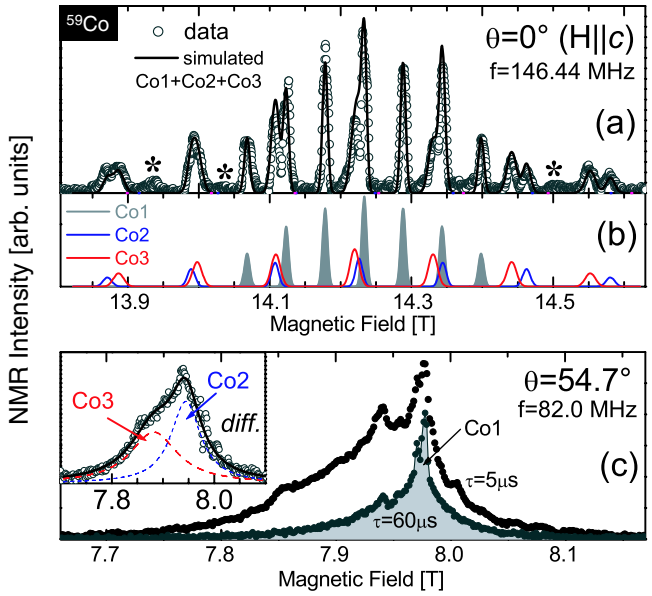

FIG. 1 (color online). (a) Spectrum for $H \parallel c$ (circles) and $T = 30$ K, with the total simulation (line) resulting from the Co1, Co2, and Co3 sites displayed in panel (b). Each site consists of seven lines split by the quadrupole frequency $^{59}\nu_c$. $\nu_c = 0.57$ MHz for Co1 is close to the value (0.68 MHz) for Co^{3+} sites in Na_1CoO_2 [24], and is distinctly lower than $\nu_c = 1.22$ MHz for Co2 and 1.14 MHz for Co3. (c) Spectrum for $\theta = 54.7°$ where the quadrupole splitting vanishes, and $T = 50$ K. Co2 and Co3 lines are much broader and more shifted than for $H \parallel c$. These two lines have a much shorter spin-spin relaxation time T_2 than the Co1 line, so they can be isolated from the latter by subtracting spectra taken at two different values of the NMR pulse spacing τ (Inset). Note that, for $\theta = 54.7°$, the Co1 line is actually split into Co1a and Co1b sublines. This effect arises from either in-plane (hyperfine or magnetic) anisotropy or from differences in the Co nearest neighbors at the Co1 sites. For simplicity, we report here only the properties of the more intense, less shifted, Co1a line (the maximum K_{iso} difference between Co1a and Co1b is 5 to 10 times smaller than the difference between the Co1 and the Co2 or Co3 sites).

then extracted from linear fits of $^{59}K_{ab,c}$ *vs.* ^{23}K data, as described in [19].

For the Co1 site, the values of the orbital shift ($K_{ab}^{orb} = 2.36\%$, $K_c^{orb} = 2.35\%$) are almost the same as those reported for the Co^{3+} site in Na_1CoO_2 [24,25]. As argued in [19,21], the isotropic character of K_{orb} is also consistent with the filled t_{2g} shell of the Co^{3+} ion. Clearly, the Co1 site corresponds to nonmagnetic Co^{3+}. This assignment may, at first sight, appear to be in contradiction with $K_{spin}(Co1) \neq 0$. We cannot rule out the possibility that the effective valence of the Co1 ion is slightly higher than +3; i.e., t_{2g} holes have a small but finite probability of residing on the Co1 sites. However, the quasi-isotropic $\mathcal{A}^{hf} = 28$ kG/μ_B, as well as the different T_1 *vs.* T behavior (see later) for this site would suggest that most of the hyperfine field may be transferred from its magnetic nearest neighbors [i.e., the second term of Eq. (1)]. Thus, it must be concluded that there are localized sites in the cobalt planes which are permanently occupied by six t_{2g} electrons.

The Co2 and Co3 sites, on the other hand, are characterized by much larger and anisotropic hyperfine fields values ($\mathcal{A}_{ab}^{hf} = 64$ and 154 kG/μ_B and $\mathcal{A}_c^{hf} = 34.5$ and 40 kG/μ_B, respectively), showing that the spin density is much larger. The difference between these sites and Co1 also manifests itself in the much larger K_{ab}^{orb} values (2.55% and 2.60%, respectively). However, the phenomenological link between K^{orb} anisotropy and the Co valence proposed in Ref. [19] appears not to hold here: K_{orb} values are similar and not strongly anisotropic for Co2 and Co3 ($K_c^{orb} = 2.37\%$ and 2.39%, respectively). Thus, while the shift difference between the Co2 and Co3 most likely arises from different electron densities at these sites, we cannot rule out the possibility that part of the difference is due to distinct *transferred* hyperfine fields from their Co nearest neighbors. If present at Co^{3+} sites, the transferred interaction should affect magnetic sites as well.

The distinction between magnetic and nonmagnetic sites is even more striking in the spin-lattice relaxation rates T_1^{-1}. $(T_1T)^{-1}$ is constant at the Co^{3+} (Co1) sites [Fig. 2(c)]. At magnetic sites, on the other hand, $(T_1T)^{-1}$ has a clear T dependence which can be ascribed to a Curie-Weiss law, typical of spin-fluctuation systems. Below ~50 K, critical fluctuations above T_M enhance T_1^{-1}, with a progressive loss of Co2 and Co3 signals.

Although a snapshot of $Na_{0.75}CoO_2$ would certainly show 75% of Co^{3+} and 25% of Co^{4+} states, this description evidently does not apply at long time scales: First, the characteristics of the magnetic sites are different from those of the highly oxidized cobalt (nominally Co^{4+}) measured in the $x = 0$ member CoO_2 [26]. Second, integration of the NMR signal intensity (corrected for T_2 decay) over the whole spectrum shows that the Co^{3+} sites represent only $30 \pm 4\%$ of the total number of sites throughout the T range. The magnitude of this number, as well as its reproducibility in different samples, demonstrates that pinning by extrinsic impurities or defects cannot explain the Co^{3+} localization. Therefore, long range magnetic order below 22 K does not arise from a minority of localized magnetic moments, as often assumed: The spin density is not concentrated on 25% of the lattice sites but is spread over ~70% of them.

A knowledge of the local magnetization in the cobalt planes allows us to compute the hyperfine field at the Na sites. Our computer simulations, an example of which is displayed in Fig. 3(c), show that any random distribution of magnetic and nonmagnetic Co sites produces a very large number of magnetically distinct ^{23}Na NMR sites, leading to a broad, featureless spectrum. This is because the ^{23}Na nuclei are coupled to a large number of Co sites: 2 (6) first neighbors and 12 (14) second neighbors for the Na(1) and

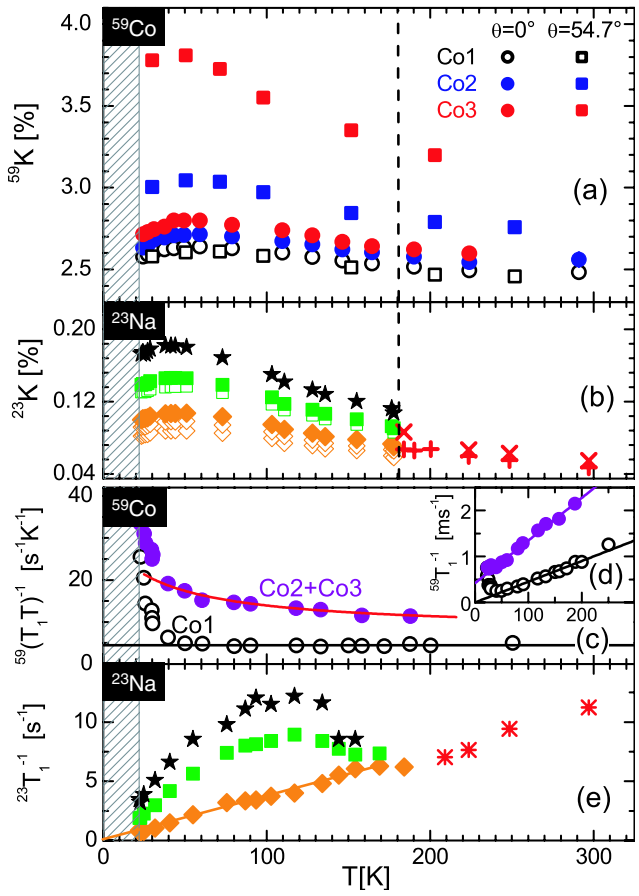

FIG. 2 (color online). (a) ^{59}K for the Co1, Co2, and Co3 sites, in two field orientations. The hatched area represents the phase with magnetic order below $T_M = 22$ K. (b) ^{23}K for $\theta = 0°$ (calibrated from the ^{23}Na resonance in aqueous NaCl solution). The vertical dashed line denotes the temperature of 180 K, where the ^{23}Na line splits. (c) $(^{59}T_1T)^{-1}$ for the Co1 and the Co2 plus Co3 signals (Co2 and Co3 central lines cannot be separated in T_1 measurements performed on central lines with $H \parallel c$). Continuous lines are fit results: $(T_1T)^{-1} = 4.5\ \mathrm{s^{-1}\,K^{-1}}$, $(T_1T)^{-1} = 8 + 800/(T + 35)\ \mathrm{s^{-1}\,K^{-1}}$. Below ~50 K, critical fluctuations above T_M enhance T_1^{-1}, with a progressive loss of Co2 and Co3 signals. (d) Corresponding T_1^{-1} data. (e) $^{23}T_1^{-1}$ data for the three main ^{23}Na lines. All T_1 values were obtained by fitting the recovery curves to standard expressions for magnetic relaxation.

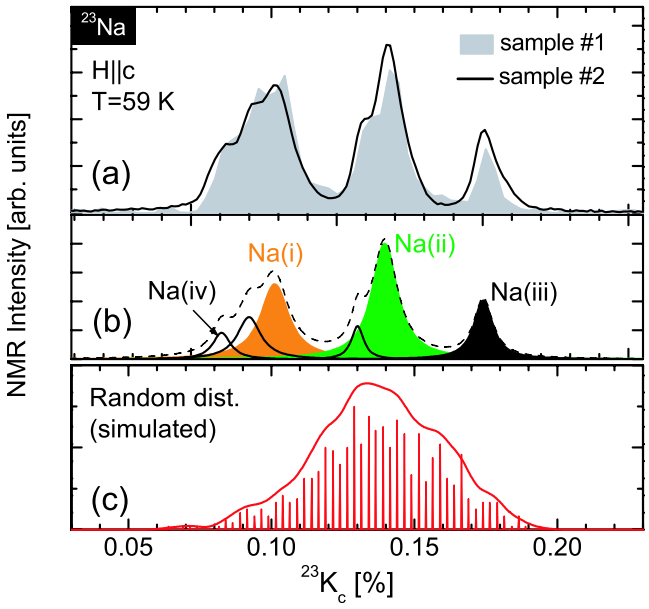

FIG. 3 (color online). (a) Central lines ($1/2 \leftrightarrow -1/2$ transitions) of the spectrum in two different single crystals at $T = 30$ K. (b) Fit to six lines, having a similar quadrupole frequency $^{23}\nu_c \simeq 1.9$ MHz to within $\pm 10\%$. (c) Simulated ^{23}Na NMR spectrum (line) obtained by a Gaussian broadening of the histogram computed for randomly distributed magnetic and nonmagnetic Co sites. Assuming two different types of magnetic sites further increases the number of lines. Hyperfine couplings to first neighbors a and to second neighbors $b = a/2$ were assumed to be identical for the Na(1) and Na(2) sites.

the Na(2) sites, respectively. These simulations are at odds with the central transitions of the ^{23}Na spectrum at $T = 59$ K, which consists of only three clearly separated main resonances, in which six lines with different K values (and negligible $^{23}\nu_c$ differences) are discernible [four of them are labeled as Na(i, . . . , iv) on Fig. 3(b)]. The small number of hyperfine fields at the Na sites demonstrates that the different Co states are spatially ordered [27]. At the same time, the specific spectral shape imposes an unprecedented set of constraints on any model of the Co and Na^+ patterns in $Na_{0.75}CoO_2$. However, computational uncertainties concerning the 3D stacking, which is crucial for ^{23}Na and ^{59}Co NMR spectra, prevent us from determining whether the in-plane pattern depicted in Fig. 4 [13], or another pattern, is correct. The problem should be solved by full DFT calculations of the Na/Co patterns and of the ^{23}Na shifts, which are underway.

Surprisingly, the ^{23}Na spectrum collapses into two very close lines above 180 K [see shifts in Fig. 2(b)], as if the cobalt planes were electronically homogeneous. However, the observation of distinct Co1, Co2, and Co3 sites above 180 K tells us that this is not the case. Thus, the averaging of the hyperfine fields must be due to Na^+ ions occupying several distinct sites within the NMR time window. The Na^+ jump frequency has to be larger than the frequency separating the NMR lines with a fine structure (~10 kHz), but smaller than the typical frequency of faster probes, such as x-ray diffraction (XRD), for which Na^+ order is already well-defined at ~250 K [15]. This direct observation of slow Na motion with localization around 180 K rationalizes the anomalies observed in the T dependence of magnetic [28], lattice [15], and possibly charge ([29] and references therein), properties of this material.

Since the NMR time scale is basically identical for ^{59}Co and ^{23}Na, the observation that Co electronic differentiation coexists above 180 K with Na motional averaging is strik-

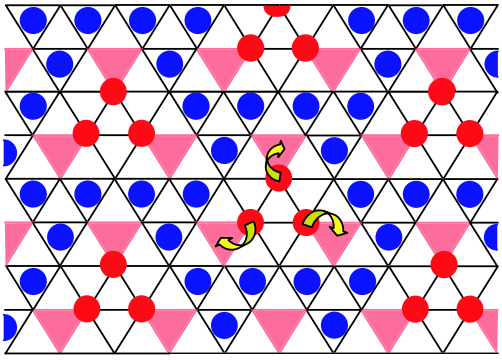

FIG. 4 (color online). Na^+ ordering pattern proposed for $x = 0.75$ in Ref. [13]. Sodium ions at Na(1) positions may hop (arrows) onto unoccupied neighboring Na(2) positions (solid triangles) but sodium ions at Na(2) positions (triangle centers) cannot because edge-sharing triangles cannot be occupied simultaneously. Our NMR data suggest a similar selective mobility in $Na_{0.75}CoO_2$.

ing. This implies either that electronic disproportionation at the Co sites is completely unrelated to the Na positions, which would contradict theoretical expectations [9–11,13], or that excursions of the Na^+ ions are sufficiently limited so that an electrostatic landscape remains well-defined at long time scales. In this event, it is likely that the formation of an electronic texture contributes to the final stabilization of the Na^+ pattern, as recent calculations indeed suggest [7].

Figure 4 illustrates one such possibility where only sodium ions at Na(1) positions may hop onto a neighboring site. Our data suggest that there is such a contrast in the behavior at the Na sites: There is actually no sign of motion for the ^{23}Na(i) site since both K and $1/T_1$ above and below 180 K follow the same trends. T_1^{-1} for this line is approximately linear in T [Fig. 2(d)], as seen for the Co^{3+} sites. This similarity strongly suggests that these ^{23}Na(i) sites are primarily coupled to the Co^{3+} sites. However, there are 18% of ^{23}Na(i) sites per unit cell (24% of the total Na intensity), so there is no simple connection with the 30% of Co^{3+} sites. On the other hand, ^{23}Na(i) + ^{23}Na(iv) sites represent 33% of the total number of Na^+ ions, suggesting that these sites may correspond to the Na(1) positions [13]. For the ^{23}Na(ii) and ^{23}Na(iii) sites, $^{23}T_1^{-1}$ *vs.* T shows a broad maximum around 100 K [Fig. 2(d)]. This relaxation peak is not seen in the T_1 data of any Co site and is probably caused by anomalous vibrations of the Na^+ ions after they have localized on the NMR time scale. We thus anticipate anomalous phonon modes, possibly analogous to rattling phonons of thermoelectric skutterudites and superconducting pyrochlores [30].

In conclusion, NMR provides a microscopic view of how Na^+ ordering impacts on both the electronic texture and the Na mobility in Na_xCoO_2. Since these are potential ingredients of the thermoelectric effect, controlling ion doping in these materials (either by dilute doping of ions of different mobility or via nanoscale electrochemical manipulations on Na_xCoO_2 surfaces [31]) should result in an improved thermoelectric performance. More generally, control of ionic textures in battery materials appears to be an exciting route for tailoring electronic properties.

This work was supported by the ANR NEMSICOM and by the IPMC Grenoble. We thank J. F. Stebbins, D. Carlier-Larregaray, Y. S. Meng, and particularly M. Roger, for useful exchanges.

*Correspondence to: Marc-Henri.Julien@ujf-grenoble.fr

[1] E. Dagotto, Science **309**, 257 (2005).
[2] K. McElroy *et al.*, Science **309**, 1048 (2005).
[3] J. Zhang *et al.*, Phys. Rev. Lett. **96**, 066401 (2006).
[4] M. L. Foo *et al.*, Phys. Rev. Lett. **92**, 247001 (2004).
[5] M. Lee *et al.*, Nat. Mater. **5**, 537 (2006).
[6] P. Zhang *et al.*, Phys. Rev. B **71**, 153102 (2005).
[7] Y. S. Meng, A. van der Ven, M. K. Y. Chan, and G. Ceder, Phys. Rev. B **72**, 172103 (2005).
[8] Y. Wang and J. Ni, Phys. Rev. B **76**, 094101 (2007).
[9] J. Merino, B. J. Powell, and R. H. McKenzie, Phys. Rev. B **73**, 235107 (2006).
[10] C. A. Marianetti and G. Kotliar, Phys. Rev. Lett. **98**, 176405 (2007).
[11] M. Gao, S. Zhou, and Z. Wang, Phys. Rev. B **76**, 180402 (2007).
[12] F. C. Chou *et al.*, arXiv:0709.0085.
[13] M. Roger *et al.*, Nature (London) **445**, 631 (2007).
[14] H. W. Zandbergen *et al.*, Phys. Rev. B **70**, 024101 (2004).
[15] J. Geck *et al.*, Phys. Rev. Lett. **97**, 106403 (2006).
[16] R. Ray *et al.*, Phys. Rev. B **59**, 9454 (1999).
[17] F. L. Ning *et al.*, Phys. Rev. Lett. **93**, 237201 (2004).
[18] M. Itoh and M. Nagawatari, Physica B (Amsterdam) **271–282**, 516 (2000).
[19] I. R. Mukhamedshin *et al.*, Phys. Rev. Lett. **94**, 247602 (2005).
[20] J. L. Gavilano *et al.*, Phys. Rev. B **74**, 064410 (2006).
[21] I. R. Mukhamedshin *et al.*, arXiv:cond-mat/0703561.
[22] C. T. Lin, D. P. Chen, A. Maljuk, and Lemmens, J. Cryst. Growth **292**, 422 (2006).
[23] J. Wooldridge, D. McK. Paul, G. Balakrishnan, and M. R. Lees, J. Phys. Condens. Matter **17**, 707 (2005).
[24] C. de Vaulx *et al.*, Phys. Rev. Lett. **95**, 186405 (2005).
[25] G. Lang *et al.*, Phys. Rev. B **72**, 094404 (2005).
[26] C. de Vaulx *et al.*, Phys. Rev. Lett. **98**, 246402 (2007).
[27] See also I. R. Mukhamedshin *et al.*, Phys. Rev. Lett. **93**, 167601 (2004), where $Co^{3+/4+}$ states were assumed.
[28] T. F. Schulze *et al.*, Phys. Rev. Lett. **100**, 026407 (2008).
[29] Y. Ishida, H. Ohta, A. Fujimori, and H. Hosono, J. Phys. Soc. Jpn. **76**, 103709 (2007).
[30] M. Yoshida *et al.*, Phys. Rev. Lett. **98**, 197002 (2007).
[31] O. Schneegans *et al.*, J. Am. Chem. Soc. **129**, 7482 (2007).